SLAC – PUB – 3965
May 1986
(A)

RADIATION OF A CHARGE IN A PERFECTLY CONDUCTING CYLINDRICAL PIPE WITH A JUMP IN ITS CROSS SECTION*

S. A. KHEIFETS

Stanford Linear Accelerator Center
Stanford University, Stanford, California, 94305

and

S. A. HEIFETS

University of Houston, University Park, Houston, Texas, 77004

ABSTRACT

Electromagnetic fields of a point charge moving on the axis of an infinitely long straight cylindrical superconducting pipe with a sudden change of its cross section are found. The longitudinal coupling impedance of this structure is calculated. The method developed can be applied to some other geometries of interest.

---

* Work supported by the Department of Energy, contract DE–AC03–76SF00515.

Contributed to the Stanford Linear Accelerator Conference,
Stanford, California June 2-6, 1986

1. INTRODUCTION

The problem of finding the electromagnetic fields created by a charge moving through various geometric structures bounded by metallic walls has an important bearing on the accelerator theory. Apart from evident need for reliable evaluation of the energy loss into higher modes, there is also an important problem of evaluating the coupling impedance due to changes in the particle environment. While for a long bunch (in comparison to the relevant dimensions of the considered structure) there are several reliable numerical codes which do the job, they rapidly become too time consuming for short bunches.

Here we present the results of calculations of electromagnetic fields radiated by a point charge moving on an axis of a cylindrical superconducting pipe with an abrupt change in its cross section. From them then we find the longitudinal coupling impedance. The geometry and the coordinate system (cylindrical) is sketched in Fig. 1. For certainty we consider the case of a charge coming out of the bigger pipe of the cross section radius a and entering the narrow pipe of the cross section radius b. The opposite case of a charge exiting from the narrow pipe and entering the bigger one can be considered in a similar way. Coupling impedance of a cross section change for a planar geometry was considered in Ref. 1.

We see three reasons for conducting the present work. First, it is useful to consider a problem theoretically since it gives better understanding of details of the radiation process for given geometry. Second, the numerical results obtained here are in a sense complimentary to purely numerical results of existing codes, providing an answer in the parameter regions which can not be reached by existing codes. Third, the results may be interesting in themselves sometimes. For example, high frequency instabilities within bunches depend on the average

coupling impedance over a broad frequency band. Hence a simple summation over an independent cross section jumps is a rather good approximation in such cases.

Besides, the case of a pipe with a flange (which is an interesting case in itself) can be obtained from our results in the limit $a \to \infty$. The approach developed here can also serve as a starting point for investigating other geometries (such as a cylindrical scraper, for example).

The current density of a point charge moving on the axis of the pipe is

$$\mathbf{j} = \mathbf{e}_r 0 + \mathbf{e}_\theta 0 + \mathbf{e}_z \frac{qc\beta}{2\pi r}\, \delta(r)\, \delta(z - c\beta t)\ , \tag{1.1}$$

where $c\beta$ is the charge velocity. If one defines the Fourier components of any vector $\mathbf{V}$ for the angular frequency ω by expression

$$\tilde{\mathbf{V}} = \frac{1}{2\pi} \int_{-\infty}^{+\infty} dt \mathbf{V} \exp(i\omega t)\ , \tag{1.2}$$

then the Fourier components of the current density is

$$\tilde{\mathbf{j}} = \mathbf{e}_r 0 + \mathbf{e}_\theta 0 + \mathbf{e}_z \frac{q\delta(r)}{2\pi r}\ \exp(ikz/\beta)\ , \tag{1.3}$$

where $\delta(r)$ is Dirac's radial δ-function.

2. ELECTROMAGNETIC FIELDS

Due to symmetry of the problem electromagnetic field has only three nonzero components:E_r, E_z, and H_θ. The Fourier components of the solutions of the Maxwell equations which satisfy the boundary condition $E_z(z) = 0$ on the pipe wall for $z < 0, r = a$ and the radiation condition at $z \to -\infty$ (conversely, condition $E_z(z) = 0$ on the pipe wall for $z > 0, r = b$ and the radiation condition at $z \to \infty$) are known.[2] The radial component is:

$$\widetilde{E}_r^- = \widetilde{E}_r^{S-} + \widetilde{E}_r^{R-} \ , \tag{2.1}$$

where the synchronous (with the particle) part of the field is

$$\widetilde{E}_r^{S-} = (q\tau/\pi c\beta)\exp(ikz/\beta)[K_1(\tau r) + I_1(\tau r)K_0(\tau a)/I_0(\tau a)] \tag{2.2}$$

and the radiated (reflected) part of the field is

$$\widetilde{E}_r^{R-} = i\Sigma_n B_n^-(\nu_n/a)J_1(\nu_n r/a)\lambda_{an}\exp(-iz\lambda_{an}) \ . \tag{2.3}$$

Analogously two other components are:

$$\widetilde{E}_z^- = \widetilde{E}_z^{S-} + \widetilde{E}_z^{R-} \ , \tag{2.4}$$

and

$$\widetilde{H}_\theta^- = \widetilde{H}_\theta^{S-} + \widetilde{H}_\theta^{R-} \ , \tag{2.5}$$

where

$$\widetilde{E}_z^{S-} = -i(q\tau/\pi c\gamma\beta)\exp(ikz/\beta)[K_0(\tau r) - I_0(\tau r)K_0(\tau a)/I_0(\tau a)] \ , \tag{2.6}$$

$$\widetilde{E}_z^{R-} = \Sigma_n B_n^- (\nu_n^2/a^2) J_0(\nu_n r/a) \exp(-iz\lambda_{an}) \tag{2.7}$$

$$\widetilde{H}_\theta^{S-} = (q\tau/\pi c) \exp(ikz/\beta)[K_1(\tau r) + I_1(\tau r) K_0(\tau a)/I_0(\tau a)] \ , \tag{2.8}$$

$$\widetilde{H}_\theta^{R-} = -ik\Sigma_n B_n^- (\nu_n/a) J_1(\nu_n r/a) \exp(-iz\lambda_{an}) \ . \tag{2.9}$$

Here $k = \omega/c$, $\tau = k/\gamma\beta$, $\gamma = 1/\sqrt{1-\beta^2}$,$K_0, K_1, I_0$ and I_1 are modified Bessel functions of the second and the first kind, respectively and of the zeroth and first order, correspondingly.J_0 and J_1 are Bessel functions of the first kind and the zeroth and the first order, correspondingly. The propagation constants λ_{an} are

$$\lambda_{an} = \sqrt{k^2 - \nu_n^2/a^2} \ , \tag{2.10}$$

with the following choice of the sign of its imaginary part (that choice is defined by the radiation condition):

$$Im\lambda_{an} > 0 \ , \tag{2.11}$$

ν_n are defined by equation $J_0(\nu_n) = 0$ and are understood to be ordered: $\nu_1 < \nu_2 < ..... < \nu_n < \nu_{n+1} ..., n = 1, 2, ...\infty$.

In the same way the Fourier components of the solutions of the Maxwell equations which satisfy the boundary condition $E_z(z) = 0$ on the pipe wall for $z > 0, r = b$ and the radiation condition at $z \to \infty$ are:

$$\widetilde{E}_r^+ = \widetilde{E}_r^{S+} + \widetilde{E}_r^{R+} \ , \tag{2.12}$$

where the synchronous part of the field is

$$\widetilde{E}_r^{S+} = (q\tau/\pi c\beta) \exp(ikz/\beta)[K_1(\tau r) + I_1(\tau r) K_0(\tau b)/I_0(\tau b)] \ , \tag{2.13}$$

and the radiated (diffracted) part of the field is

$$\widetilde{E}_r^{R+} = -i\Sigma_n B_n^+(\nu_n/b)J_1(\nu_n r/b)\lambda_{bn}\exp(iz\lambda_{bn}) \ . \tag{2.14}$$

Analogously two other components are:

$$\widetilde{E}_z^+ = \widetilde{E}_z^{S+} + \widetilde{E}_z^{R+} \ , \tag{2.15}$$

and

$$\widetilde{H}_\theta^+ = \widetilde{H}_\theta^{S+} + \widetilde{H}_\theta^{R+} \ , \tag{2.16}$$

where

$$\widetilde{E}_z^{S+} = -i(q\tau/\pi c\gamma\beta)\exp(ikz/\beta)[K_0(\tau r) - I_0(\tau r)K_0(\tau b)/I_0(\tau b)] \ , \tag{2.17}$$

$$\widetilde{E}_z^{R+} = \Sigma_n B_n^+(\nu_n^2/b^2)J_0(\nu_n r/b)\exp(iz\lambda_{bn}) \ , \tag{2.18}$$

$$\widetilde{H}_\theta^{S+} = (q\tau/\pi c)\exp(ikz/\beta)[K_1(\tau r) + I_1(\tau r)K_0(\tau b)/I_0(\tau b)] \ , \tag{2.19}$$

$$\widetilde{H}_\theta^{R+} = -ik\Sigma_n B_n^+(\nu_n/b)J_1(\nu_n r/b)\exp(iz\lambda_{bn}) \ . \tag{2.20}$$

The propagation constants λ_{bn} are defined by

$$\lambda_{bn} = \sqrt{k^2 - \nu_n^2/b^2} \ , \tag{2.21}$$

with the same choice of the sign of its imaginary part

$$Im\lambda_{bn} > 0 \ . \tag{2.22}$$

In all equations above $B_n^\pm$ are unknown coefficients to be defined by the boundary and continuity conditions in the plane $z = 0$.

Each term in the expressions for the diffracted field describes either a *nth* wave propagating in the positive z direction, if $k > \nu_n/a$, or an evanescent wave, if $k < \nu_n/a$. Similarly, each term in the expressions for the reflected field describes either a *nth* wave propagating in the negative z direction, if $k > \nu_n/b$, or an evanescent wave, if $k < \nu_n/b$. For any given k there are finite number of the propagating and infinite number of evanescent waves.

3. BOUNDARY AND CONTINUITY CONDITIONS

On a perfectly conducting wall the tangential component of the electric field should be zero. In our case that means that the radial component of electric field for all $b < r < a$ should be zero at $z = 0$. For the charge entering the narrow pipe

$$\widetilde{E}_r^-(r,0) = 0 \ . \tag{3.1}$$

Conversely, for the charge exiting the narrow pipe

$$\widetilde{E}_r^+(r,0) = 0 \ . \tag{3.2}$$

In the plane $z = 0$ but in the opening of the pipe all the fields components should be continuous:

For $0 < r < b$

$$\widetilde{E}_r^+(r,0) = \widetilde{E}_r^-(r,0) \ , \tag{3.3}$$

$$\widetilde{E}_z^+(r,0) = \widetilde{E}_z^-(r,0) \ , \tag{3.4}$$

$$\widetilde{H}_\theta^+(r,0) = \widetilde{H}_\theta^-(r,0) \ . \tag{3.5}$$

Since three functions E_r, E_z and H_θ are not arbitrary but are solutions of Maxwell equations one of them (3.4) or (3.5) is redundant. It is sufficient to solve the system of two equations, for example (3.3),(3.4).

At this point it is convenient to introduce the following notations

$$\kappa = ka \ , \tag{3.6}$$

$$p = b/a \ , \tag{3.7}$$

$$u = \tau a = ka/\beta\gamma \ , \tag{3.8}$$

$$M = qk/\pi c\gamma^2\beta^2 \ , \tag{3.9}$$

$$G_1(r,d) = K_1(\tau r) + I_1(\tau r)K_0(\tau d)/I_0(\tau d) \ , \tag{3.10}$$

$$G_0(r,d) = K_0(\tau r) - I_0(\tau r)K_0(\tau d)/I_0(\tau d) \ , \tag{3.11}$$

where $d = a$ or b, then

$$\widetilde{E}_r^+ = \gamma M G_1(r,b)\exp(ikz/\beta) - i\Sigma_n B_n^+(\nu_n/b)J_1(\nu_n r/b)\lambda_{bn}\exp(iz\lambda_{bn}) \ , \tag{3.12}$$

$$\widetilde{E}_z^+ = -iMG_0(r,b)\exp(ikz/\beta) + \Sigma_n B_n^+(\nu_n^2/b^2)J_0(\nu_n r/b)\exp(iz\lambda_{bn}) \ , \tag{3.13}$$

$$\widetilde{H}_\theta^+ = \gamma\beta MG_1(r,b)\exp(ikz/\beta) - ik\Sigma_n B_n^+(\nu_n/b)J_1(\nu_n r/b)\exp(iz\lambda_{bn}) \ , \tag{3.14}$$

$$\widetilde{E}_r^- = \gamma M G_1(r,a)\exp(ikz/\beta) + i\Sigma_n B_n^-(\nu_n/a)J_1(\nu_n r/a)\lambda_{an}\exp(-iz\lambda_{an}) \ , \tag{3.15}$$

$$\widetilde{E}_z^- = -iMG_0(r,a)\exp(ikz/\beta) + \Sigma_n B_n^-(\nu_n^2/a^2)J_0(\nu_n r/a)\exp(-iz\lambda_{an}) \ , \tag{3.16}$$

$$\widetilde{H}_\theta^- = \gamma\beta MG_1(r,a)\exp(ikz/\beta) - ik\Sigma_n B_n^-(\nu_n/a)J_1(\nu_n r/a)\exp(-iz\lambda_{an}) \ . \tag{3.17}$$

Substitute now these expressions into equations (3.3),(3.4) and obtain the following system of equations which define unknown coefficients $B_n^{\pm}$:

$$\Sigma_n B_n^+ \frac{\nu_n^2}{b^2} J_0(\nu_n r/b) = iM[G_1(r,b) - G_1(r,a)] + \Sigma_n B_n^- \frac{\nu_n^2}{a^2} J_0(\nu_n r/a) \ , \qquad (3.18)$$

$$\Sigma_n B_n^- \frac{\nu_n}{a} J_1(\nu_n r/a)\lambda_{an}$$

$$= \begin{cases} i\gamma M G_1(r,a), & \text{if } b < r < a \ ; \\ -i\gamma M[G_1(r,b) - G_1(r,a)] - \Sigma_n B_n^+ \frac{\nu_n}{b} J_1(\nu_n r/b)\lambda_{bn}, & \text{if } r < b \ . \end{cases} \qquad (3.19)$$

The system of transcendental equations (3.18),(3.19) can be transferred into a system of linear algebraic equations by using the following property of orthogonality of Bessel functions on the interval $0, d$:

$$\int_0^d r dr J_0(\nu_n r/d) J_0(\nu_m r/d) = \delta_{nm} d^2 J_1^2(\nu_n)/2 \ . \qquad (3.20)$$

To be able to use the orthogonality one needs first to substitute equation (3.19) containing the first order Bessel functions by equivalent equation containing the zero order Bessel functions. This is achieved by means of integration equation (3.19) from r to a:

$$\Sigma_n B_n^- J_0(\nu_n r/a)\lambda_{an}$$

$$= \begin{cases} i\frac{\gamma M}{r} G_0(r,a), & \text{if } b < r < a \ ; \\ -i\frac{\gamma M}{r}[G_0(r,b) - G_0(r,a)] - \Sigma_n B_n^+ J_0(\nu_n r/b)\lambda_{bn}, & \text{if } r < b \ . \end{cases} \qquad (3.21)$$

Using orthogonality (3.20) on the interval $0, b$ in equation (3.18) one gets:

$$B_m^+ = d_m + \Sigma_n f_{mn} B_n^- \ , \tag{3.23}$$

where

$$d_m = \frac{2iM}{\nu_m^2 J_1^2(\nu_m)} \int_0^b r dr J_0(\nu_m r/b)[G_0(r,b) - G_0(r,a)] \ , \tag{3.24}$$

$$f_{mn} = \frac{2\nu_n^2}{\nu_m^2 a^2 J_1^2(\nu_m)} \int_0^b r dr J_0(\nu_n r/a) J_0(\nu_m r/b) \ . \tag{3.25}$$

Using orthogonality (3.20) on the interval $0, a$ in equation (3.21) one gets:

$$B_l^- \lambda_{al} J_1^2(\nu_l) = D_l - \Sigma_n \frac{\lambda_{bn} \nu_n^2 J_1^2(\nu_n)}{\nu_l^2} f_{nl} B_n^+ \ , \tag{3.26}$$

where

$$D_l = \frac{-2iM\gamma}{\tau a^2} [\int_0^b r dr J_0(\nu_l r/a) G_0(r,b) - \int_0^a r dr J_0(\nu_l r/a) G_0(r,a)] \ . \tag{3.27}$$

The same equation (3.26) can be obtained using condition (3.5) instead of (3.4).

It is instructive to consider two limiting cases. If there is no jump, *i.e.*, $b = a$, then it is easy to see that for all n $B_n^+ = B_n^- = 0$ and there is no radiation.

In the opposite limit when the pipe is closed, i.e. $b = 0$, $E_r^- = 0$ for all $0 < r < a$, or:

$$\Sigma_n B_n^- \nu_n J_1(\nu_n r/a) \sqrt{\kappa^2 - \nu_n^2} = iMa^2 \gamma G_1(r,a) \ . \tag{3.28}$$

This equation can be solved exactly. Use, for example, the Kneser-Sommerfeld formula for *zeroth* order Bessel functions:[3]

$$\Sigma_{n=1}^{\infty} \frac{J_0(\nu_n x) J_0(\nu_n X)}{(u^2+\nu_n^2) J_1^2(\nu_n)} = \frac{I_0(xu)}{2I_0(u)} [I_0(u)K_0(Xu) - I_0(Xu)K_0(u)] \ , \qquad (3.29)$$

where $0 \leq x \leq X \leq 1, J_0(\nu_n) = 0$.

Take derivative over X

$$\Sigma_{n=1}^{\infty} \frac{\nu_n J_0(\nu_n x) J_1(\nu_n X)}{(u^2+\nu_n^2) J_1^2(\nu_n)} = \frac{u I_0(xu)}{2} [K_1(Xu) + I_1(Xu)K_0(u)/I_0(u)] \ . \qquad (3.30)$$

Comparing (3.30) and (3.28) for $b \to 0$ one gets

$$B_n^- = \frac{2iM\gamma a^2}{u(u^2+\nu_n^2) J_1^2(\nu_n)\sqrt{\kappa^2-\nu_n^2}} \ . \qquad (3.31)$$

This expression gives the radiation field produced in the Faraday cap.

4. RADIATION FIELD IN THE ULTRARELATIVISTIC LIMIT

Equations (3.23) and (3.26) constitute an (infinite) system of linear algebraic equations for unknown coefficients $B_n^{\pm}$. We will solve it in the most interesting ultrarelativistic case $\gamma \to \infty$.

Introduce dimensionless coefficients g by the following expressions:

$$B_m^{\pm} = \frac{2iqa}{\pi c} g_m^{\pm} \ . \qquad (4.1)$$

Excluding g_n^+ from (3.23) we obtain system of equations for g_n^- only:

$$\Sigma_m [T_{lm} + \delta_{lm} \widetilde{\lambda}_{al} J_1^2(\nu_l)] g_m^- = F_l \ , \qquad (4.2)$$

where

$$F_l = J_0(\nu_l p)/\nu_l^2 \ , \tag{4.3}$$

$$T_{lm} = 4\nu_m^2 p^3 J_0(\nu_m p) J_0(\nu_l p) \Sigma_n \frac{\widetilde{\lambda}_{bn}}{(\nu_n^2 - \nu_m^2 p^2)(\nu_n^2 - \nu_l^2 p^2)} \ , \tag{4.4}$$

$$\widetilde{\lambda}_{al} = \sqrt{\kappa^2 - \nu_l^2} \ , \tag{4.5}$$

$$\widetilde{\lambda}_{bl} = \sqrt{p^2\kappa^2 - \nu_l^2} \ . \tag{4.6}$$

Notice that both diffracted and reflected fields are limited for $\gamma \to \infty$ since $B_n^{\pm}$ do not depend on energy in this limit.

Up to now all the relations are exact. Since we have no means for solving the infinite system (4.2) exactly, its approximate numerical solution is used. The system is truncated to a finite size and coefficients $g_m^{\pm}$ are found by matrix inversion. Table 1 gives an idea of the coefficients behavior as a function of their sequential number n for an example of a solution for an intermediate value $p = 0.3$,$\kappa = 10.0$ and the matrix size 20x20. The approximate expressions for the electromagnetic field components are then obtained using truncated expressions from Section 2. Figs.2 - 7 illustrate how the boundary and continuity conditions are satisfied by the same approximate solution. The discontinuity of the E_r at the sharp corner of the boundary can never be approximated by any finite numbers of eigenfunctions. Nevertheless in all other regions the solution seems to be quite satisfactory.

5. LONGITUDINAL COUPLING IMPEDANCE

The longitudinal coupling impedance can be obtained by integrating the synchronous component of E_z at $r = 0$ (*i.e.*, along the particle path).[4,5] In the ultrarelativistic limit $\gamma \to \infty$:

$$Z(k) = -\frac{2\pi}{q} \int_{-\infty}^{\infty} dz \widetilde{E}_z(r = 0, z) \exp(-ikz) \ . \tag{5.1}$$

The synchronous term of E_z^S gives the following expression for the impedance per unit length:

$$dZ^S(k)/dz = \frac{2iqk}{c\gamma^2\beta^2} \ln \frac{a}{b} \ . \tag{5.2}$$

This term goes to zero in the ultrarelativistic limit.

From the radiation part of the field E_z^R after performing the integration and some algebra we get:

$$Z_{in}(k) = -Z_0/\pi p \left[\Sigma_n g_n^+ \left(\kappa p + \sqrt{\kappa^2 p^2 - \nu_n^2} \right) - p \Sigma_n g_n^- \left(\kappa - \sqrt{\kappa^2 - \nu_n^2} \right) \right] \ , \tag{5.3}$$

where $4\pi/c = Z_0 = 377$ Ohm is the impedance of the free space.

The impedance for the case of a charge exiting the narrow pipe can be found from a similar formula:

$$Z_{out}(k) = -Z_0/\pi p [\Sigma_n g_n^+ (\kappa p - \sqrt{\kappa^2 p^2 - \nu_n^2}) - p \Sigma_n g_n^- (\kappa + \sqrt{\kappa^2 - \nu_n^2})] \ . \tag{5.4}$$

Figures 8-12 present real and Figs. 13–17 imaginary parts of longitudinal impedances Z_{in} and Z_{out} for $p = 0.9, 0.7, 0.5, 0.3$, and 0.1 as functions of the normalized frequency $\kappa = a\omega/c$. The resonance behavior of the impedance is clearly exhibited.

A wake function for a Gaussian bunch

$$I(\tau) = qc/\sqrt{2\pi}a \exp(-z_0^2/2\sigma^2)$$

can be found from the impedance by integration:

$$W(z_0) = qc/4\pi^2 a \int_0^{+\infty} d\kappa \exp(-\kappa^2\sigma^2/2)[ReZ_{in}(\kappa)\cos(\kappa z_0) + ImZ_{in}(\kappa)\sin(\kappa z_0)] \quad (5.5)\ ,$$

z_0 is distance behind the bunch and σ is the bunch spread in units of a. If q is measured in *Coulombs*, then W will be measured in *Volts*. Fig. 18 gives an example of a wake function calculated by using expression (5.5) for a Gaussian bunch with the longitudinal spread $\sigma = 1.0$.

Acknowledgments

Discussions with W. Panofsky, P. Wilson, K. Bane, B. Lippmann, B. Warnock, M. Sands, P. Morton, A. Hoffmann, J. D. Jackson and R. Helm were helpful while preparing this paper. We are grateful to all of them.

REFERENCES

1. H. G. Hereward, "Coupling Impedance of a Cross-section Change for High Frequencies," CERN/ISR-D1/75-47 (October 1975).
2. J. A. Stratton, "Electromagnetic Theory," N.Y., McGraw-Hill, 1941
3. G. N. Watson, "A Treatise on the Theory of Bessel Functions," Cambridge, England, Cambridge University Press, 1944, Section 15.42, Note that formula here contains several misprints.
4. A. Chao, "Coherent Instabilities of a Relativistic Bunched Beam," SLAC–PUB–2946 (June 1982).
5. S. Kheifets, L. Palumbo and V. G. Vaccaro, "Longitudinal Impedance of a Semi-Infinite Circular Waveguide," CERN LEP-TH/85-23 (June 1985).

Table 1

N	Reg_n^+	Img_n^+	Reg_n^-	Img_n^-
1	0.7363D-02	0.9023D-02	0.5694D-01	-0.8929D-03
2	-0.1253D-02	0.1742D-02	0.1269D-01	-0.1919D-02
3	0.4227D-03	-0.7277D-03	-0.5915D-02	-0.3148D-02
4	-0.2110D-03	0.4150D-03	-0.1447D-02	0.8925D-02
5	0.1291D-03	-0.2831D-03	-0.2652D-04	0.2717D-02
6	-0.9410D-04	0.2394D-03	0.3668D-03	-0.3403D-03
7	0.8954D-04	-0.2110D-03	0.3192D-03	-0.1242D-02
8	-0.5988D-04	0.1336D-03	0.1007D-03	-0.8242D-03
9	0.4316D-04	-0.9365D-04	-0.8543D-04	-0.4475D-04
10	-0.3249D-04	0.6931D-04	-0.1417D-03	0.4291D-03
11	0.2523D-04	-0.5322D-04	-0.8227D-04	0.4134D-03
12	-0.2008D-04	0.4201D-04	0.1407D-04	0.1064D-03
13	0.1630D-04	-0.3389D-04	0.7093D-04	-0.1765D-03
14	-0.1345D-04	0.2784D-04	0.6088D-04	-0.2423D-03
15	0.1125D-04	-0.2321D-04	0.9319D-05	-0.1083D-03
16	-0.9531D-05	0.1960D-04	-0.3624D-04	0.7196D-04
17	0.8158D-05	-0.1674D-04	-0.4397D-04	0.1522D-03
18	-0.7047D-05	0.1443D-04	-0.1638D-04	0.9466D-04
19	0.6138D-05	-0.1255D-04	0.1864D-04	-0.2765D-04
20	-0.5385D-05	0.1100D-04	0.3281D-04	-0.1079D-03

FIGURE CAPTIONS

Fig. 1. Geometry of the problem and the coordinate system (a) Incoming charge, (b) Outgoing charge.

Fig. 2. An example showing how the continuity and boundary conditions are fulfilled by the real part of the radial electrical field component on the negative and on the positive sides of a jump (the truncated matrix size is 20x20, the ratio of the small to the large radii is 0.3)

Fig. 3. The same as in Fig. 2 but for the imaginary part of the radial electric field component

Fig. 4. The same as in Fig. 2 but for the real part of the longitudinal electric field component

Fig. 5. The same as in Fig. 2 but for the imaginary part of the longitudinal electric field component

Fig. 6. The same as in Fig. 2 but for the real part of the azimuthal magnetic field component

Fig. 7. The same as in Fig. 2 but for the imaginary part of the azimuthal magnetic field component

Fig. 8 The real parts of the longitudinal coupling impedances as a function of frequency [$\kappa = a\omega/c$,$p = b/a = 0.9$: (1) real part, Z_{in} (2) real part, Z_{out}, matrix size in 60×60].

Fig. 9 The same as on Fig. 8 but for $p = 0.7$.

Fig. 10 The same as on Fig. 8 but for $p = 0.5$.

Fig. 11 The same as on Fig. 8 but for $p = 0.3$.

Fig. 12 The same as on Fig. 8 but for $p = 0.1$.

Fig. 13 The imaginary parts of the longitudinal coupling impedances as a function of frequency [$\kappa = a\omega/c$,$p = b/a = 0.9$ (1) real part, (2) imaginary part, for Z_{in} and Z_{out} are represented by the same curve, matrix size in 60×60].

Fig. 14 The same as on Fig. 12 but for $p = 0.7$.

Fig. 15 The same as on Fig. 12 but for $p = 0.5$.

Fig. 16 The same as on Fig. 12 but for $p = 0.3$.

Fig. 17 The same as on Fig. 12 but for $p = 0.1$.

Fig. 18 An example of the wake function for incoming bunch with a Gaussian longitudinal charge distribution with $\sigma = a$ [$p = 0.3$; (1) wake function, (2) charge distribution].

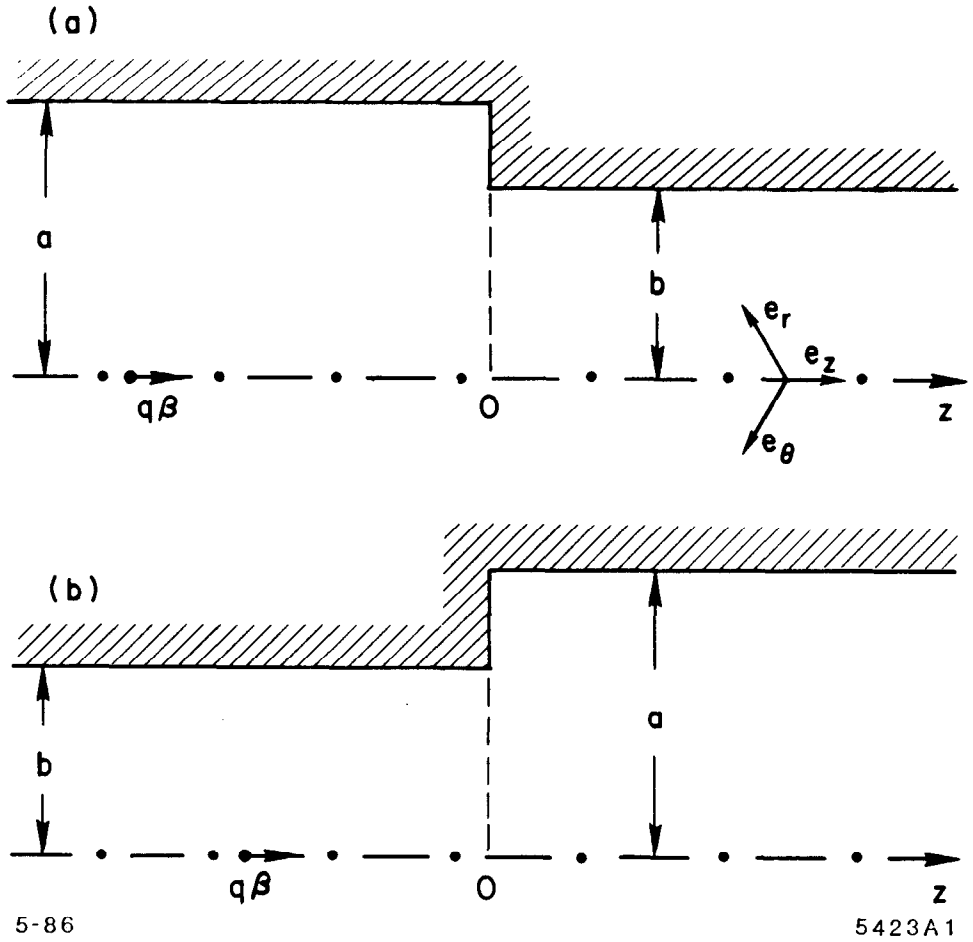

Fig. 1

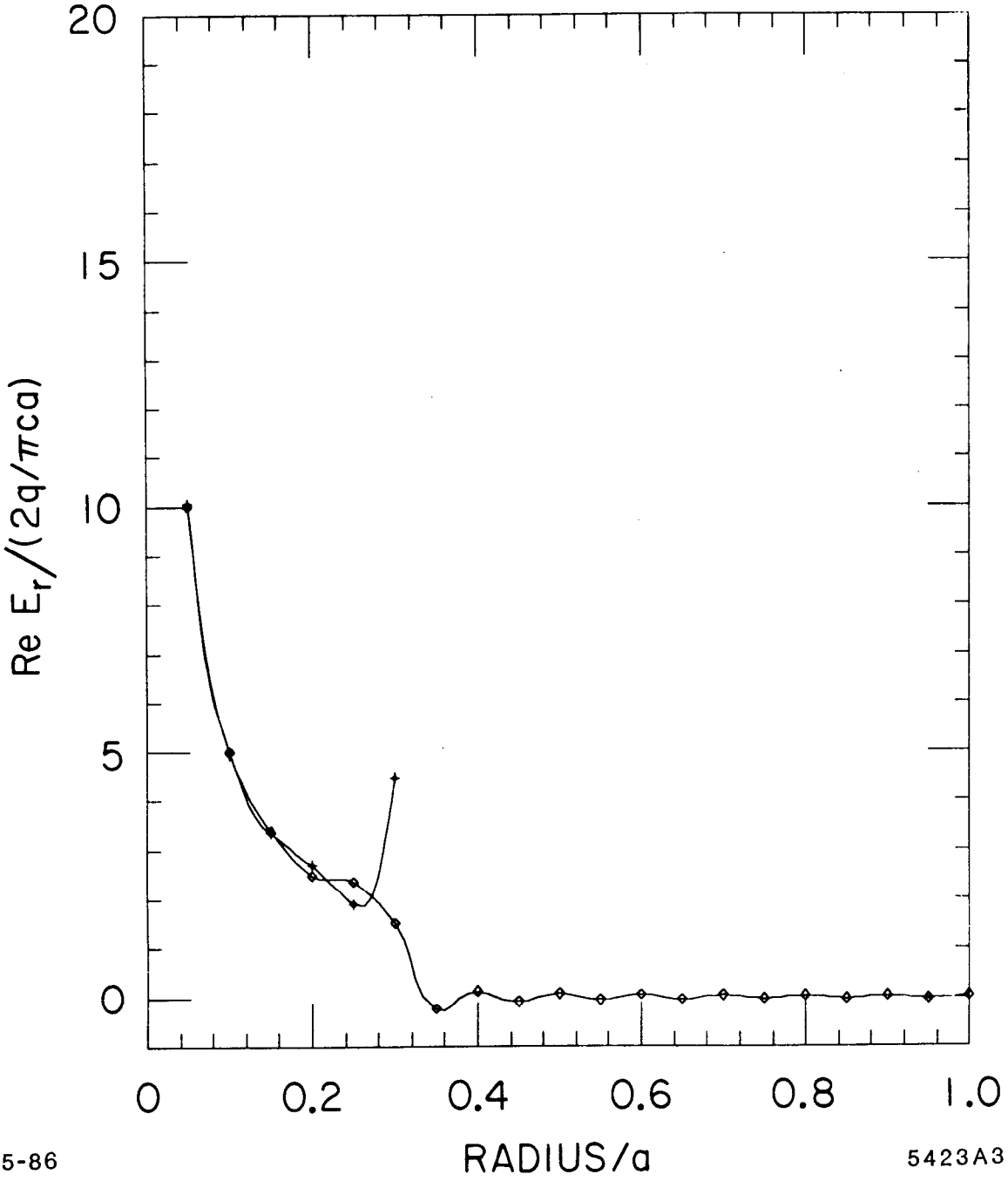

Fig. 2

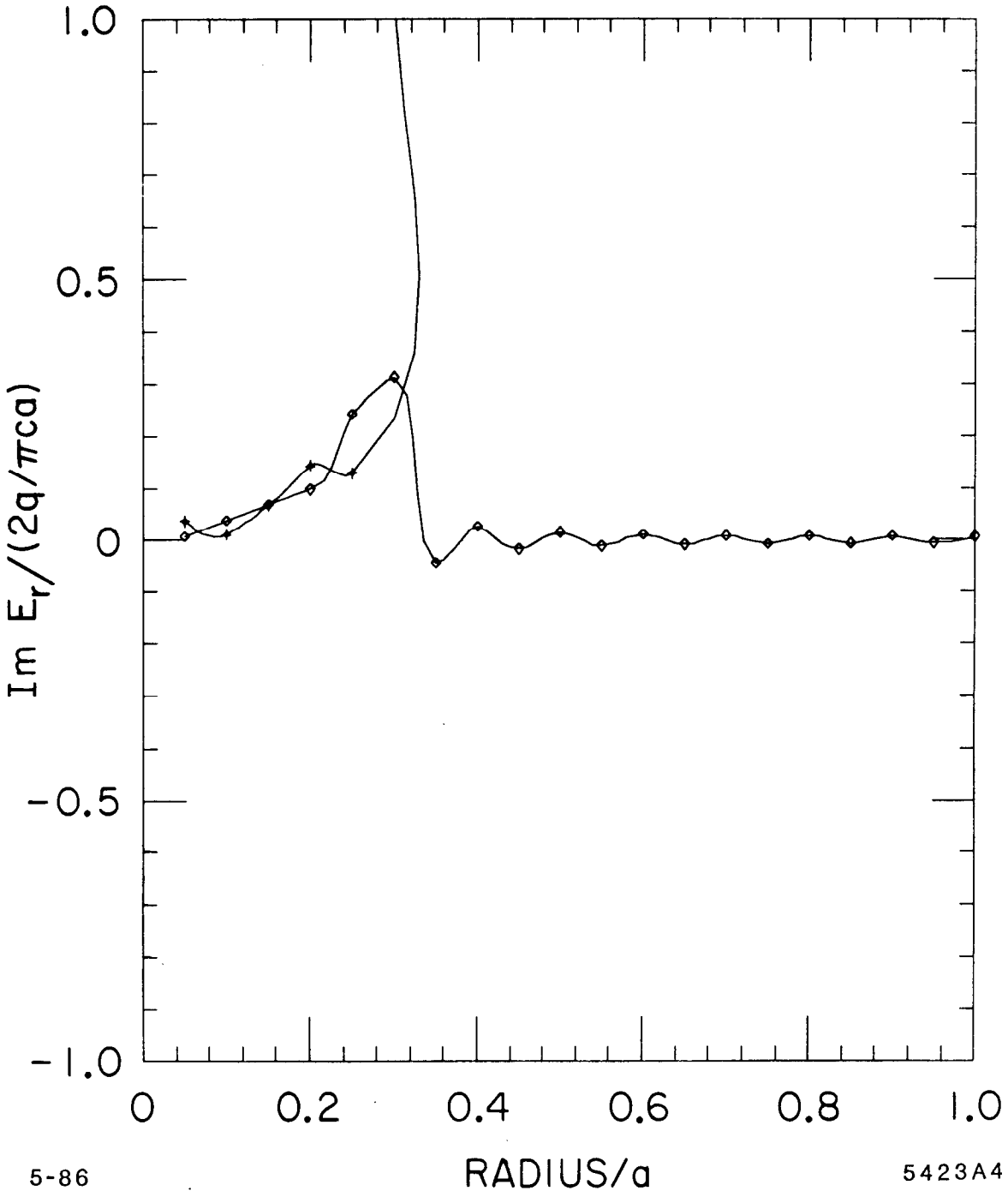

Fig. 3

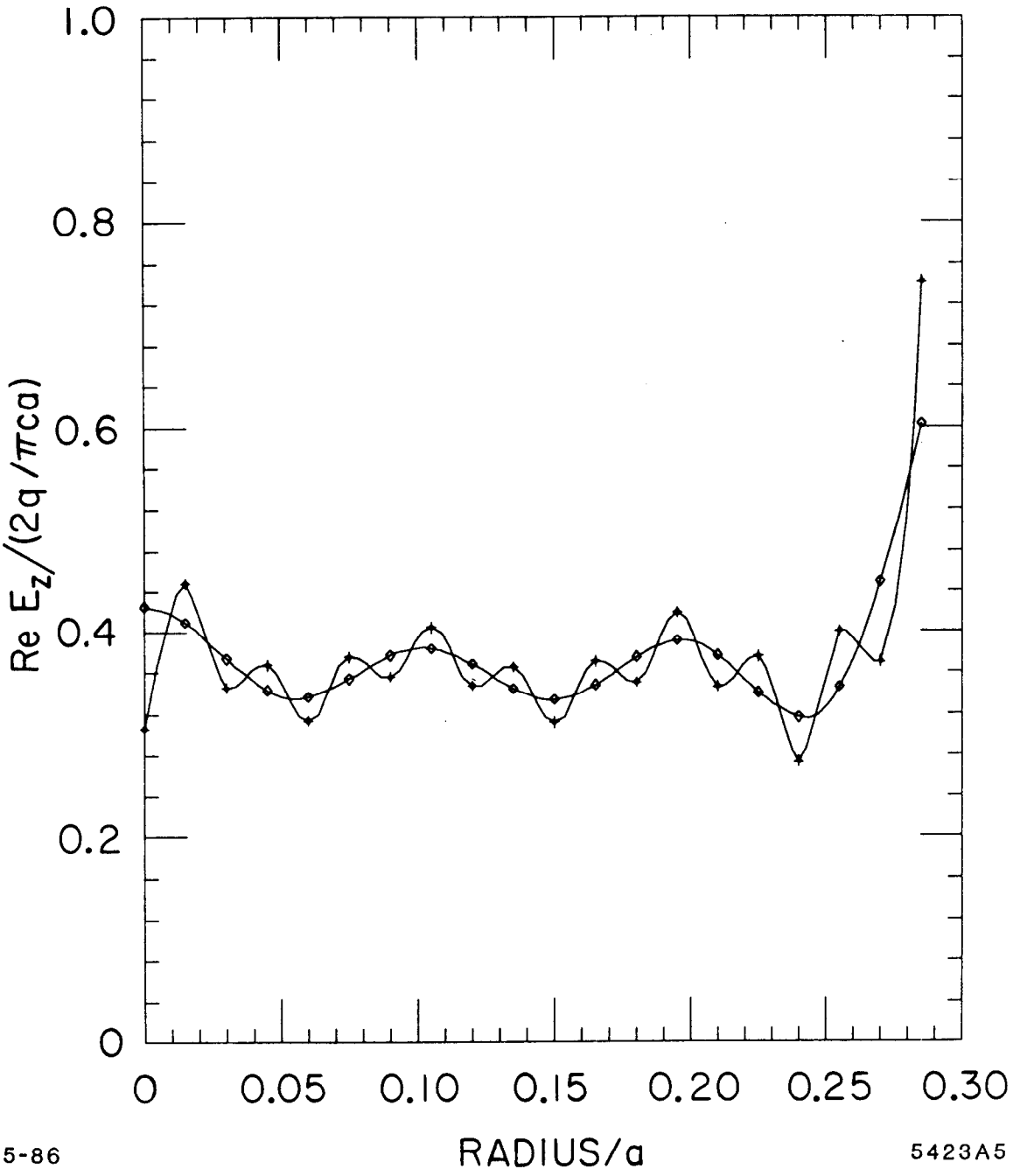
1.0
0.8
0.6
0.4
0.2
0
Re $E_z/(2q/\pi ca)$
0
0.05
0.10
0.15
0.20
0.25
0.30
RADIUS/a
5-86
5423A5

Fig. 4

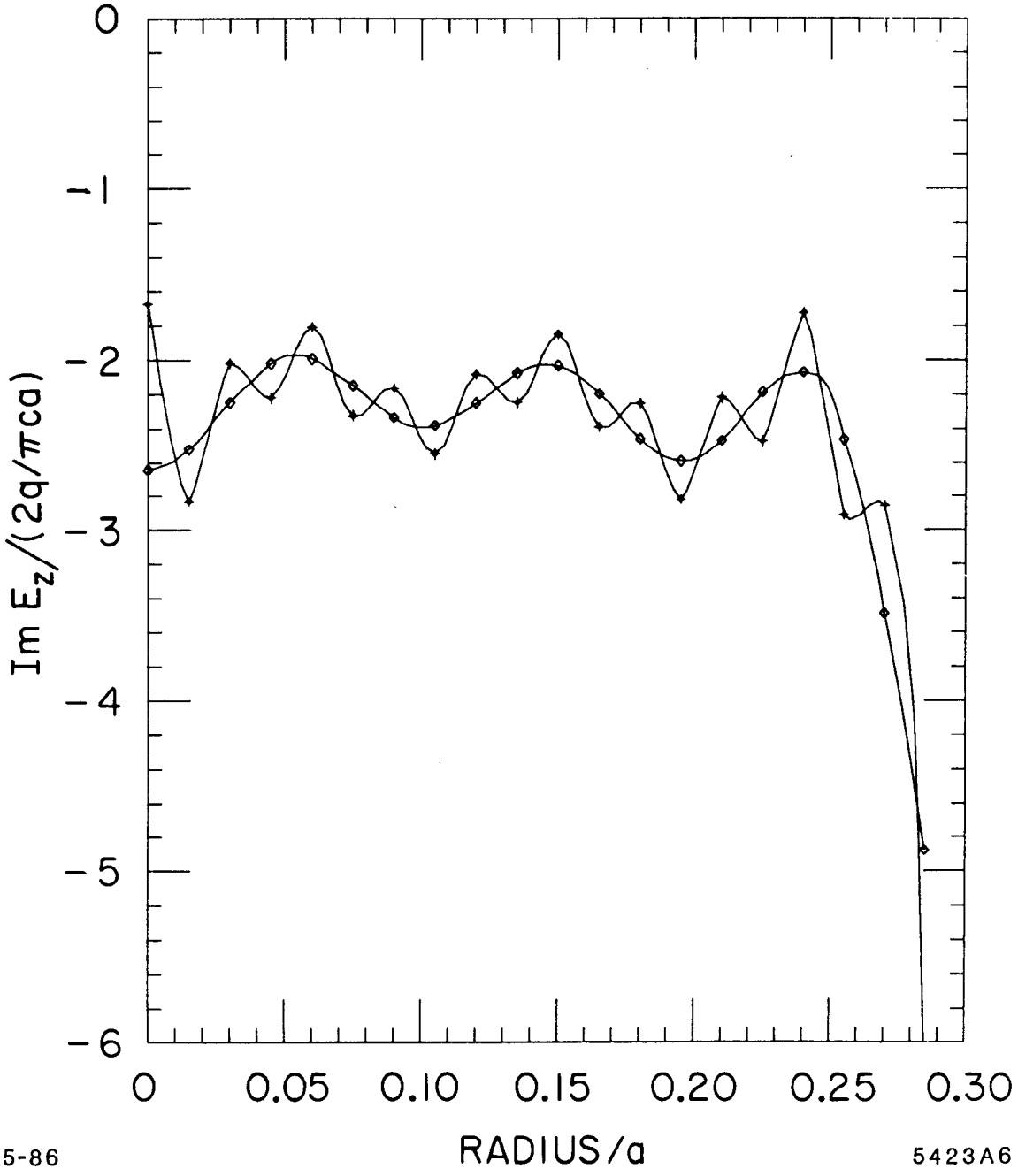
0
-1
-2
-3
-4
-5
-6
Im $E_z/(2q/\pi ca)$
0
0.05
0.10
0.15
0.20
0.25
0.30
RADIUS/a
5-86
5423A6

Fig. 5

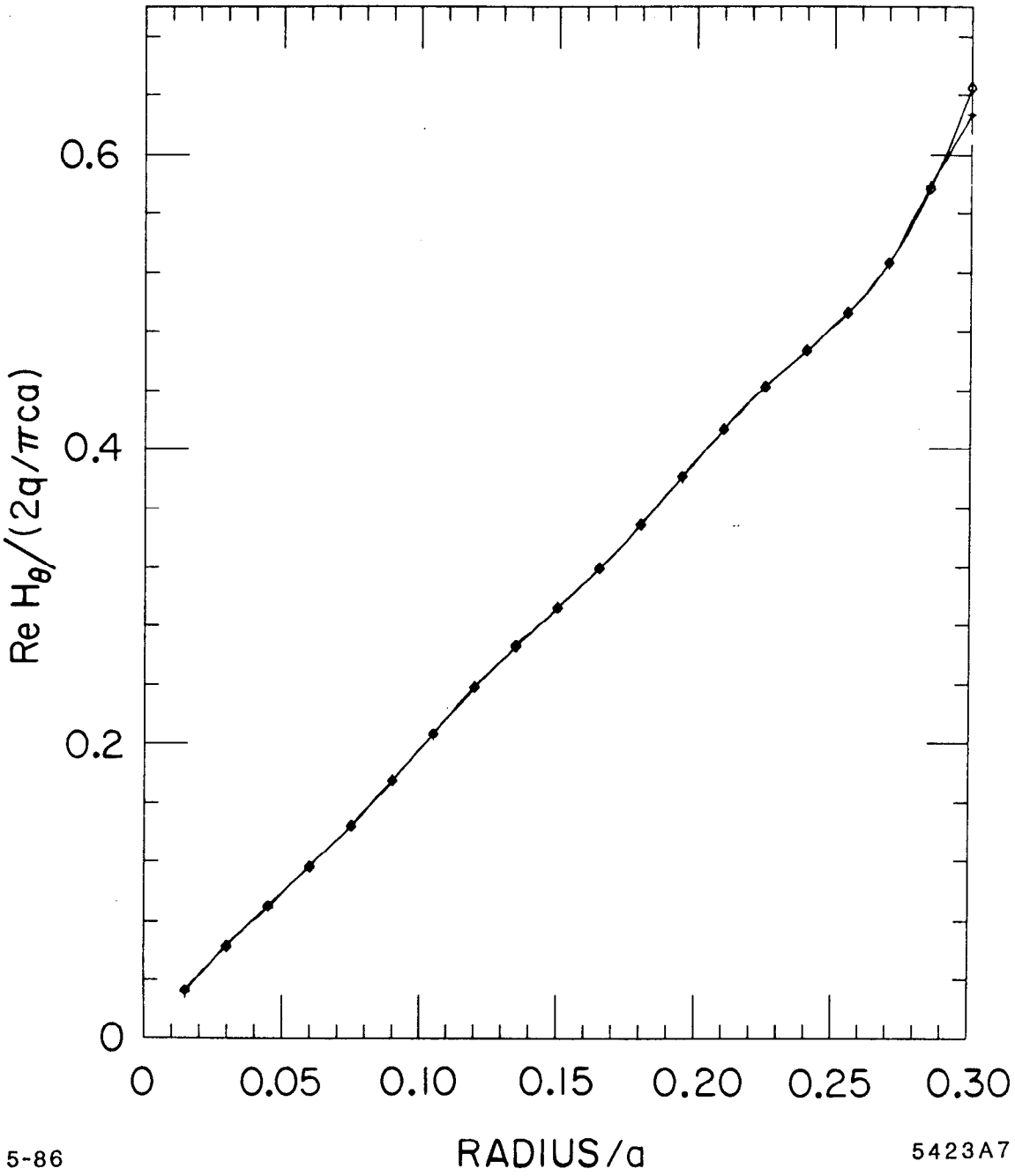
0.6
0.4
0.2
0
Re $H_\theta/(2q/\pi ca)$
0
0.05
0.10
0.15
0.20
0.25
0.30
RADIUS/a
5-86
5423A7

Fig. 6

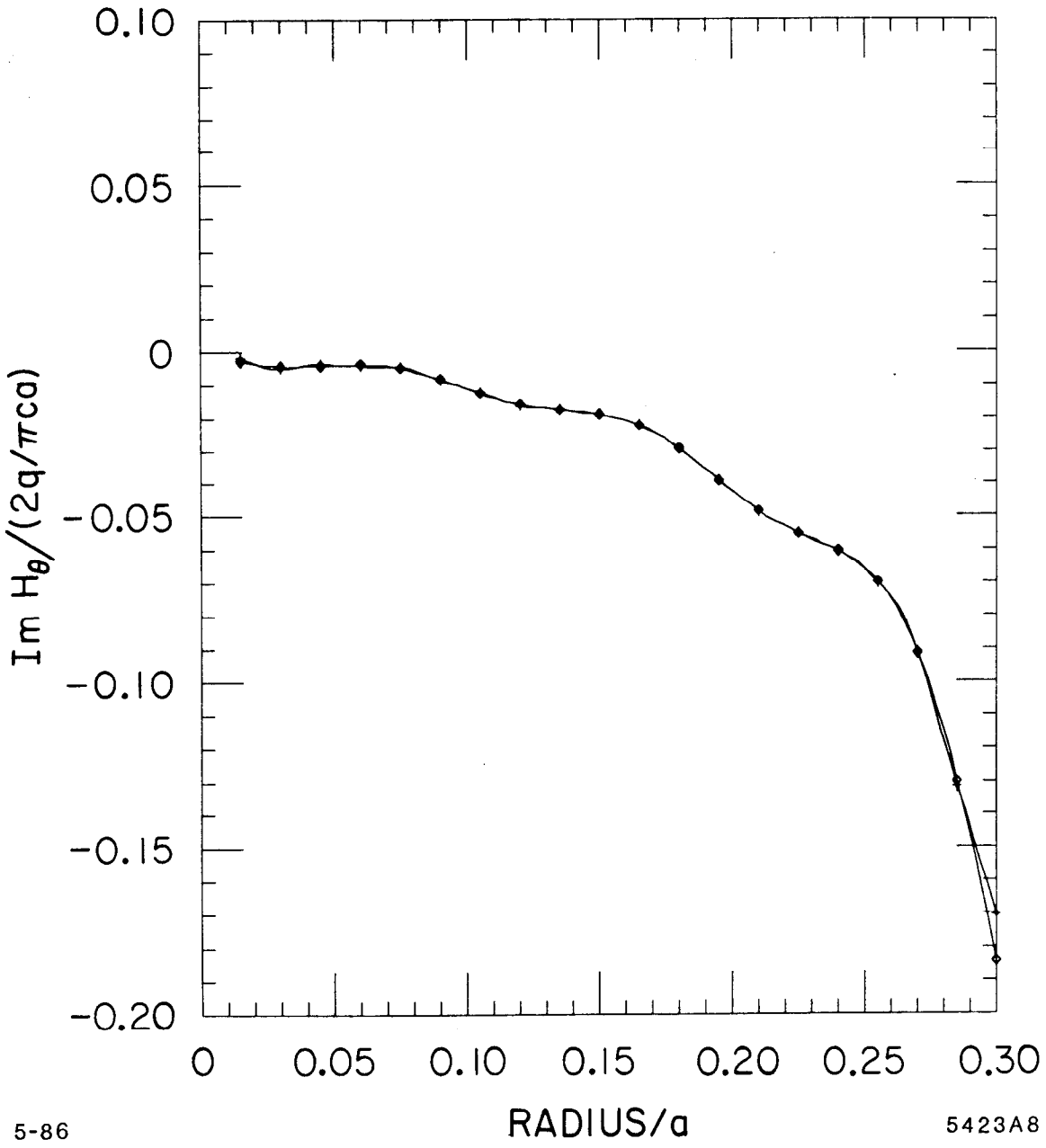
0.10
0.05
0
-0.05
-0.10
-0.15
-0.20
Im $H_\theta/(2q/\pi ca)$
0
0.05
0.10
0.15
0.20
0.25
0.30
RADIUS/a
5-86
5423A8

Fig. 7

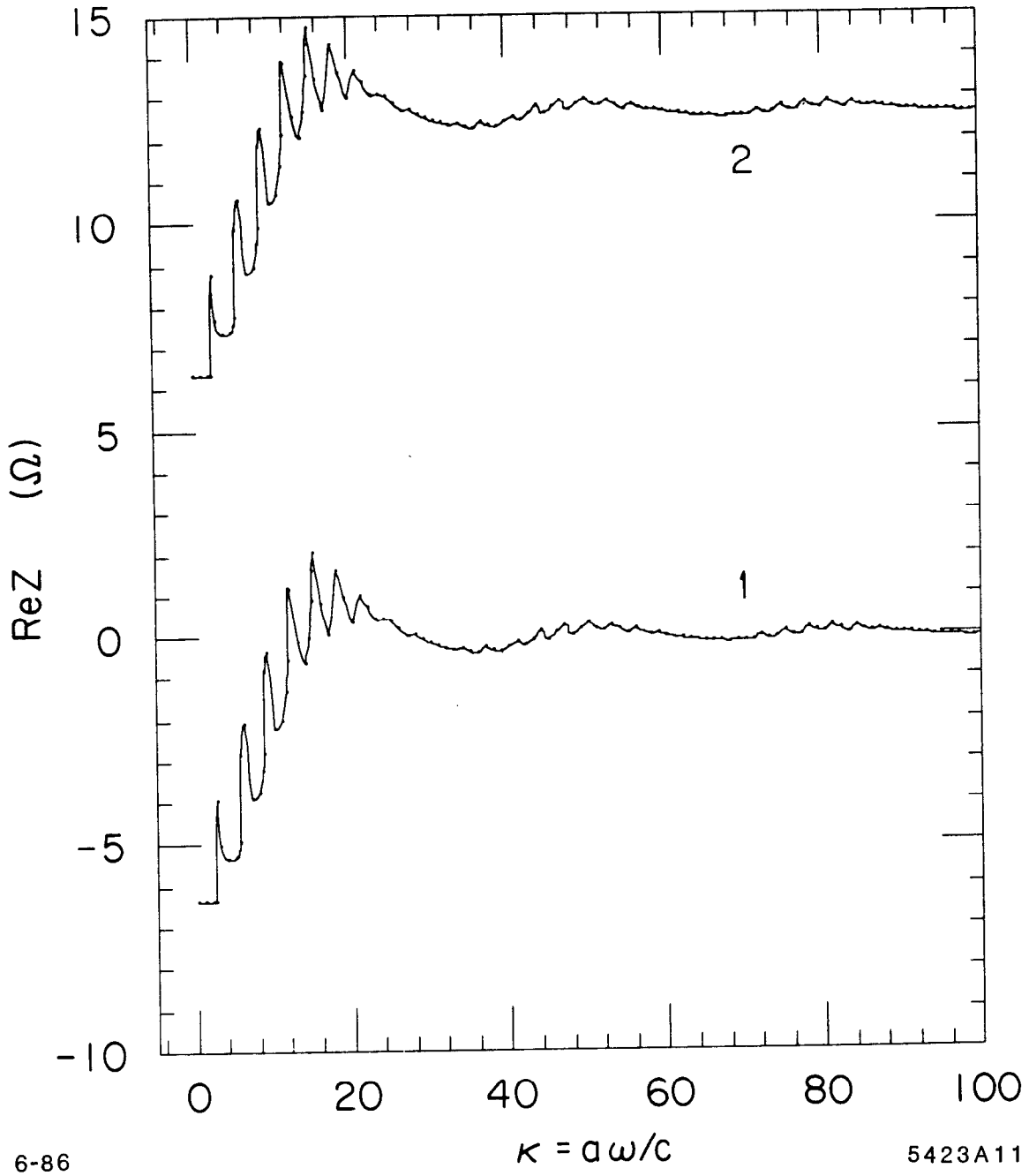

Fig. 8

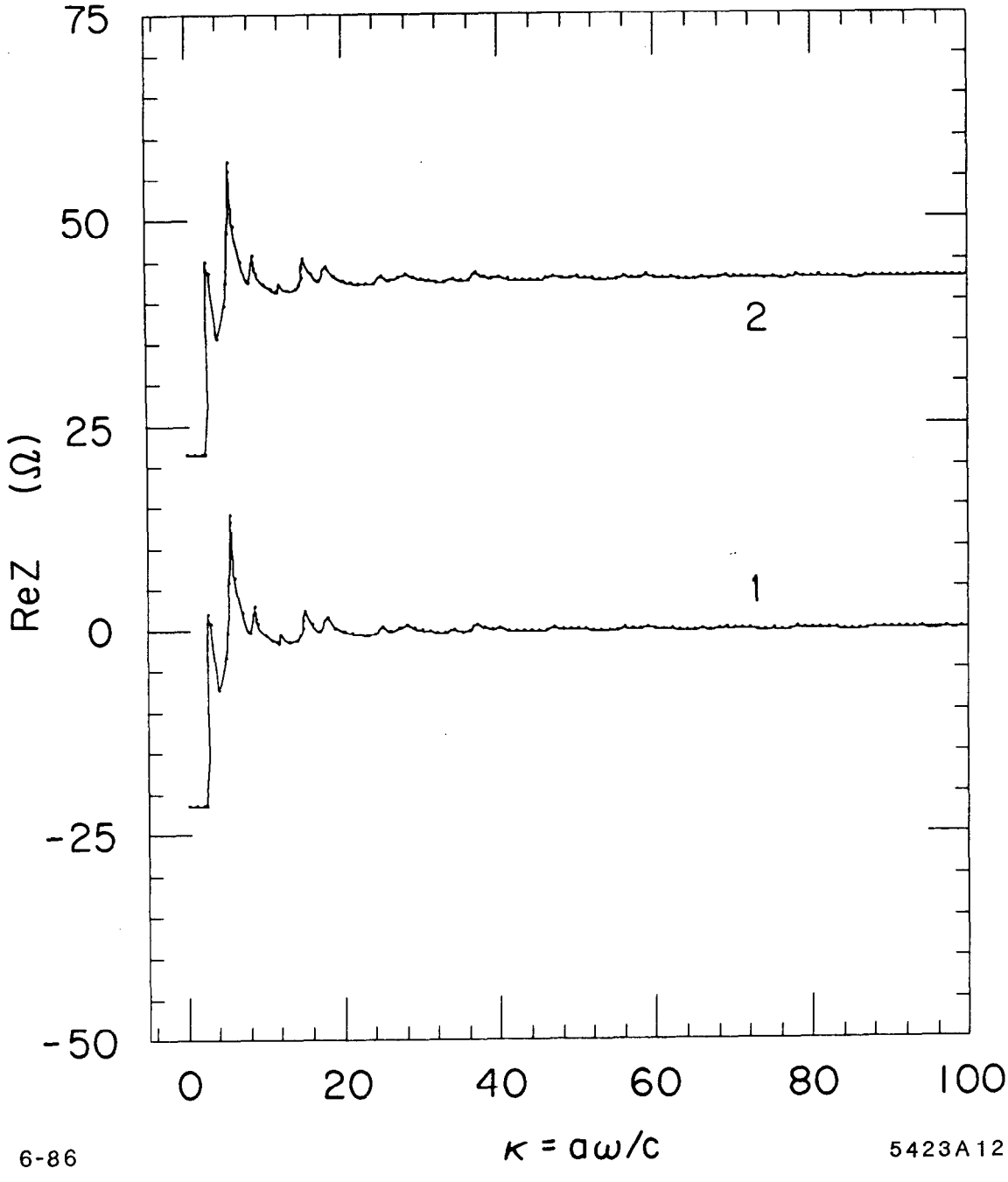

Fig. 9

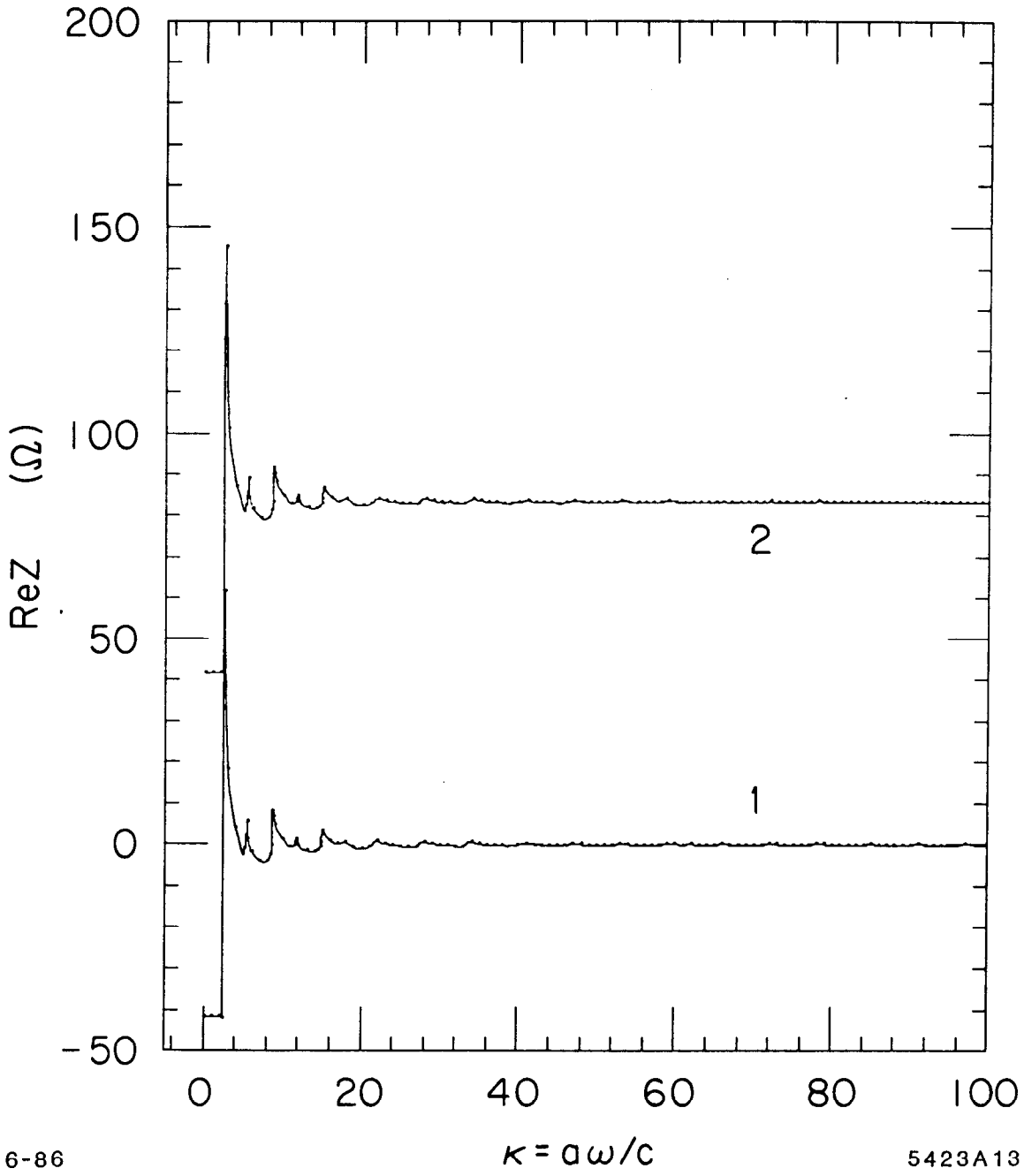

Fig. 10

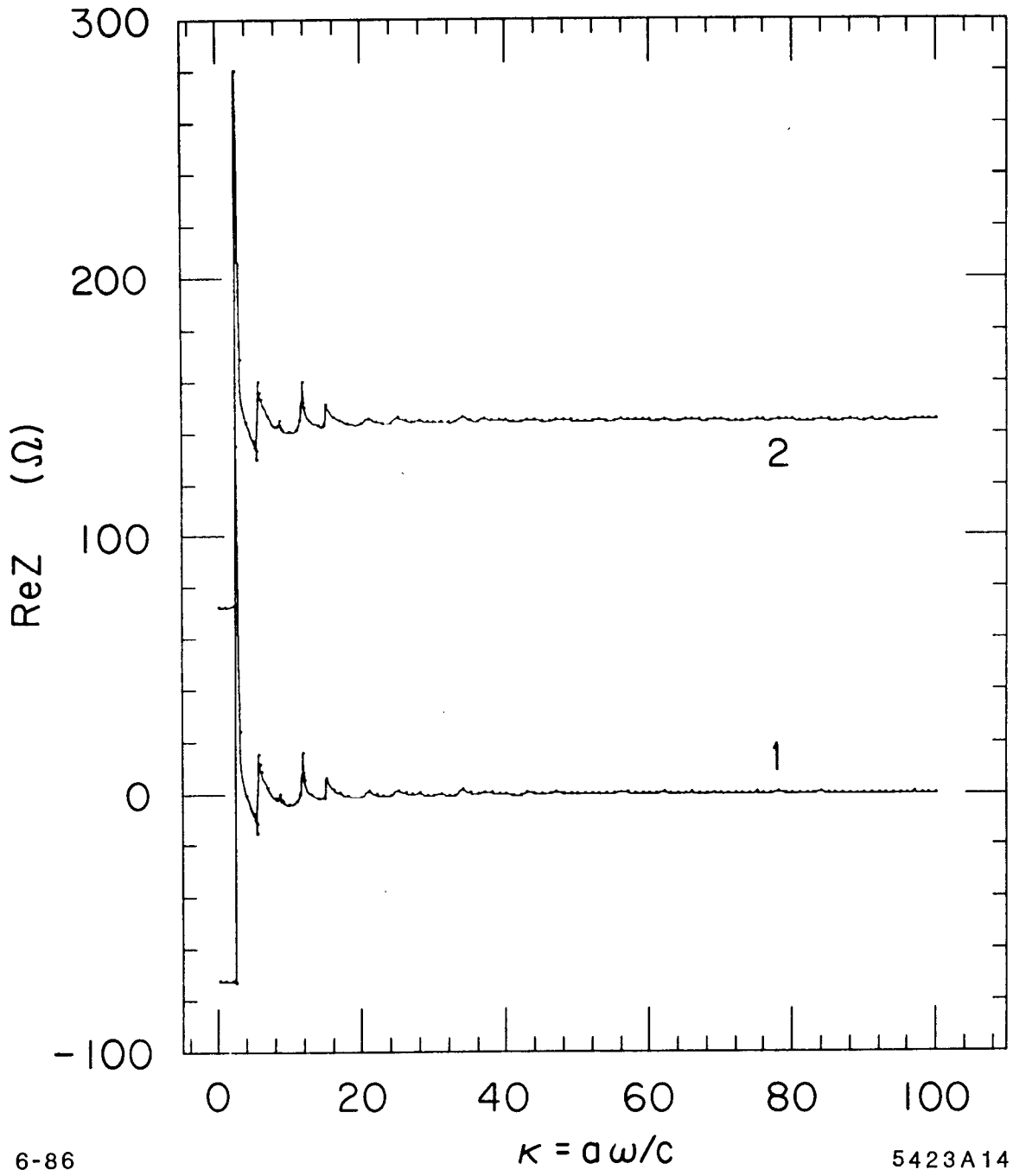

Fig. 11

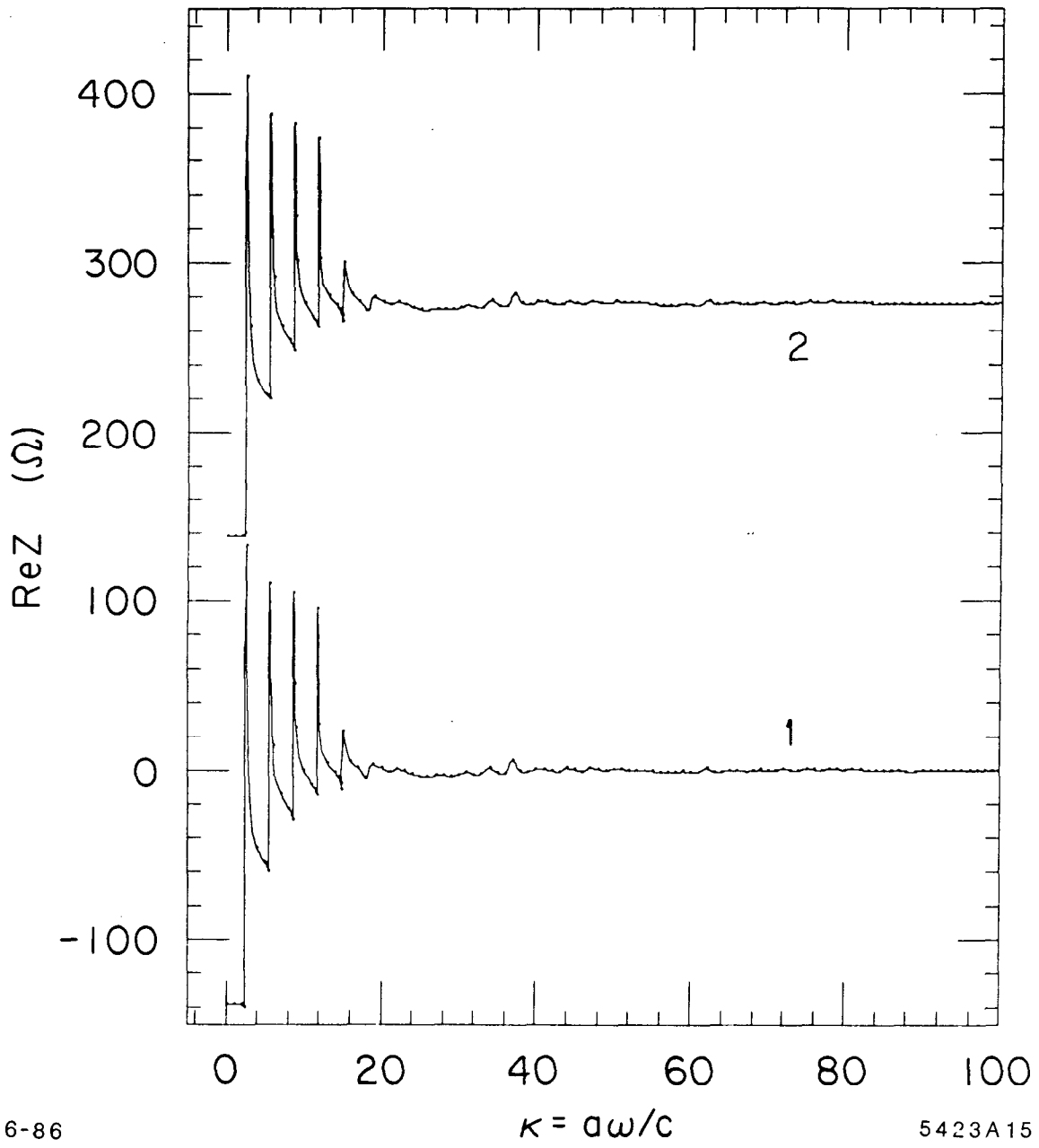

Fig. 12

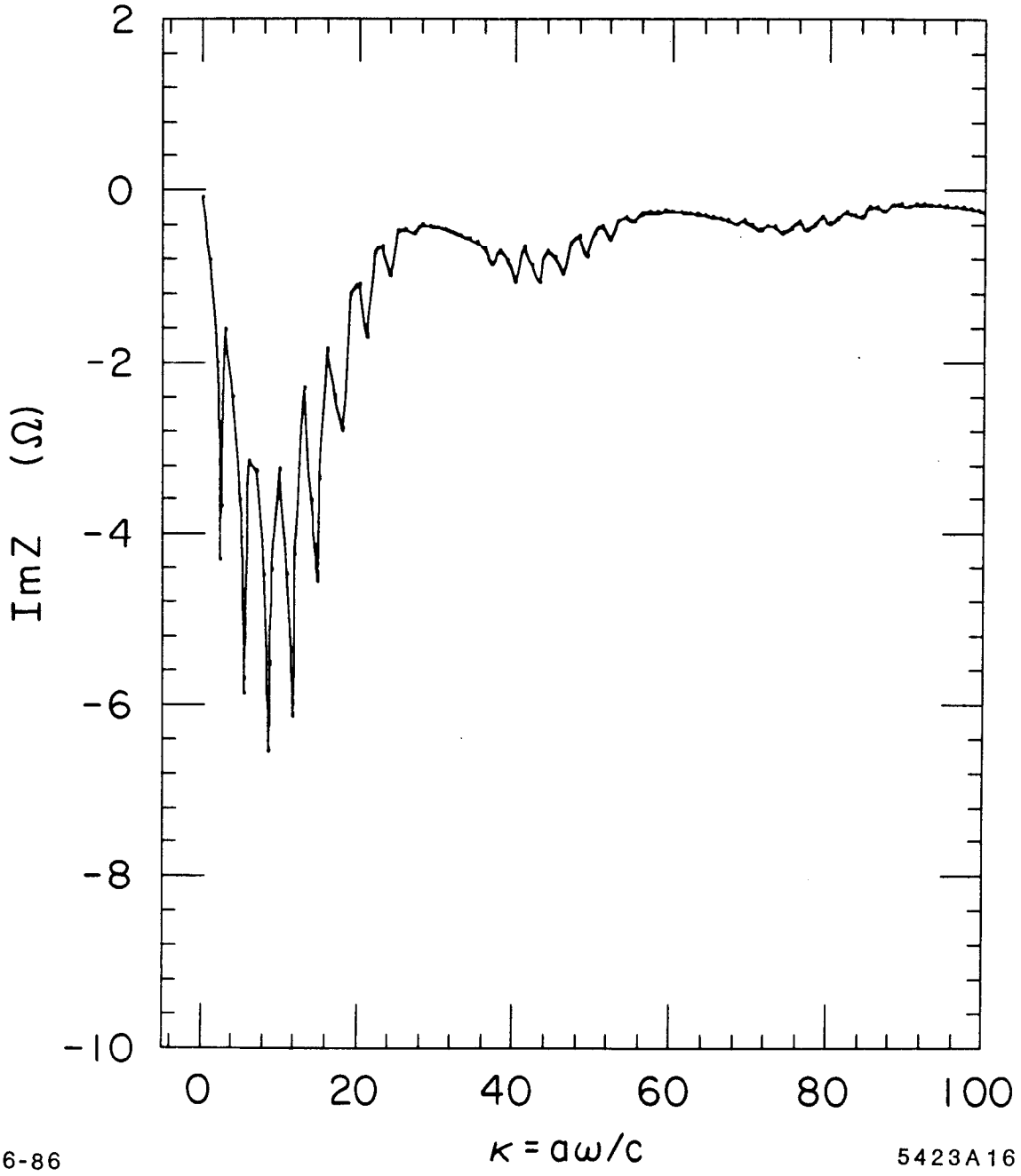

Fig. 13

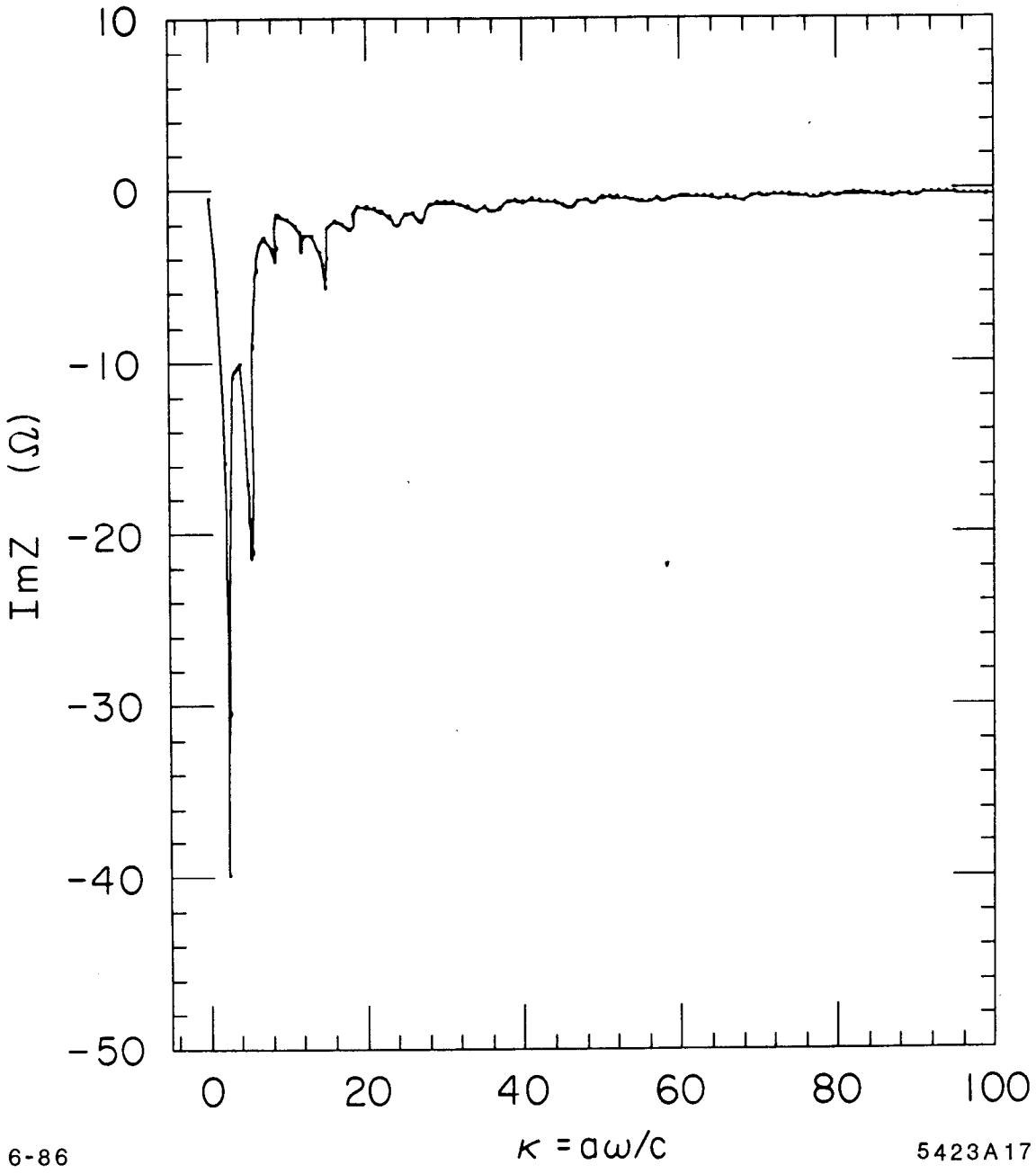

Fig. 14

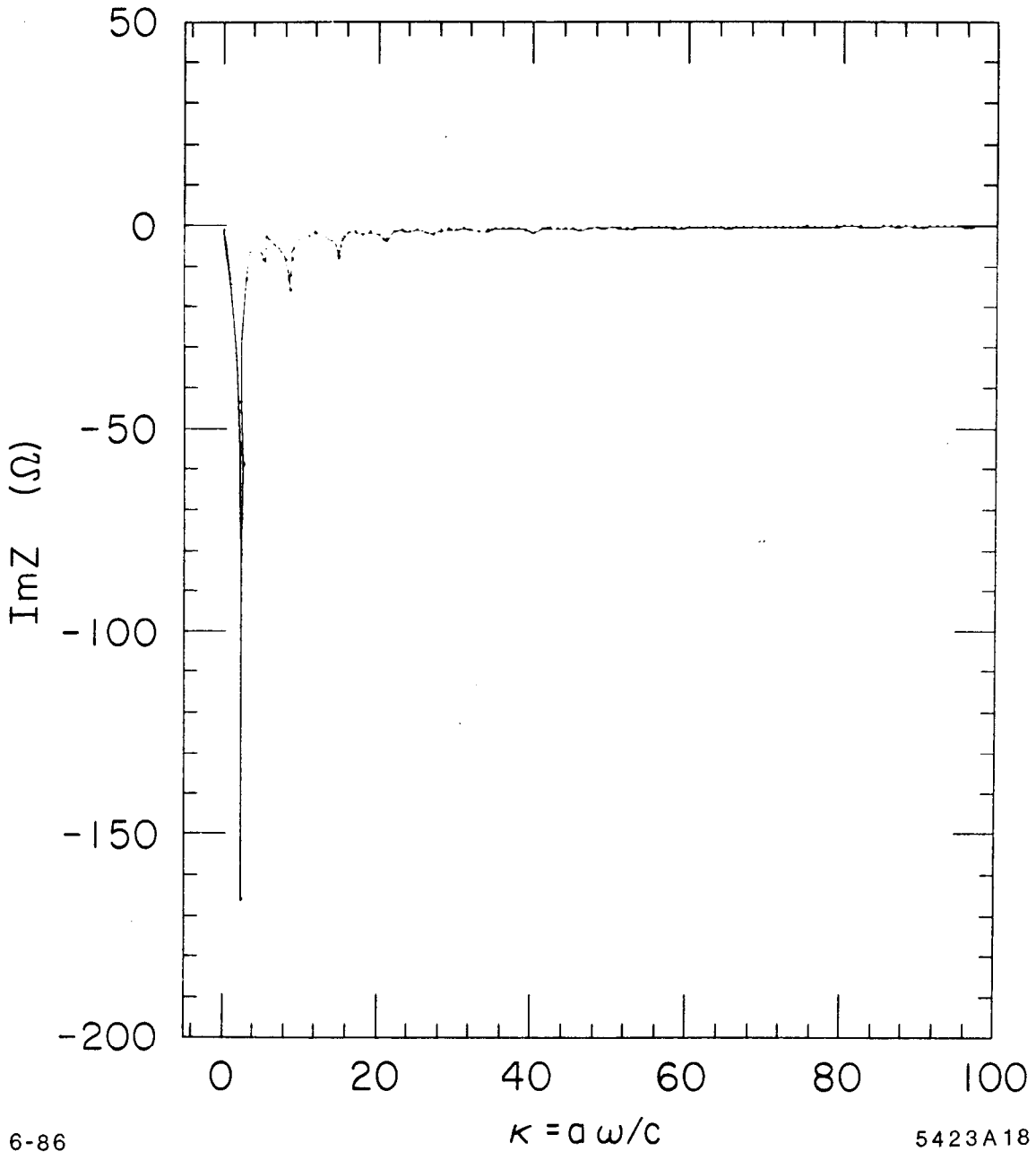

Fig. 15

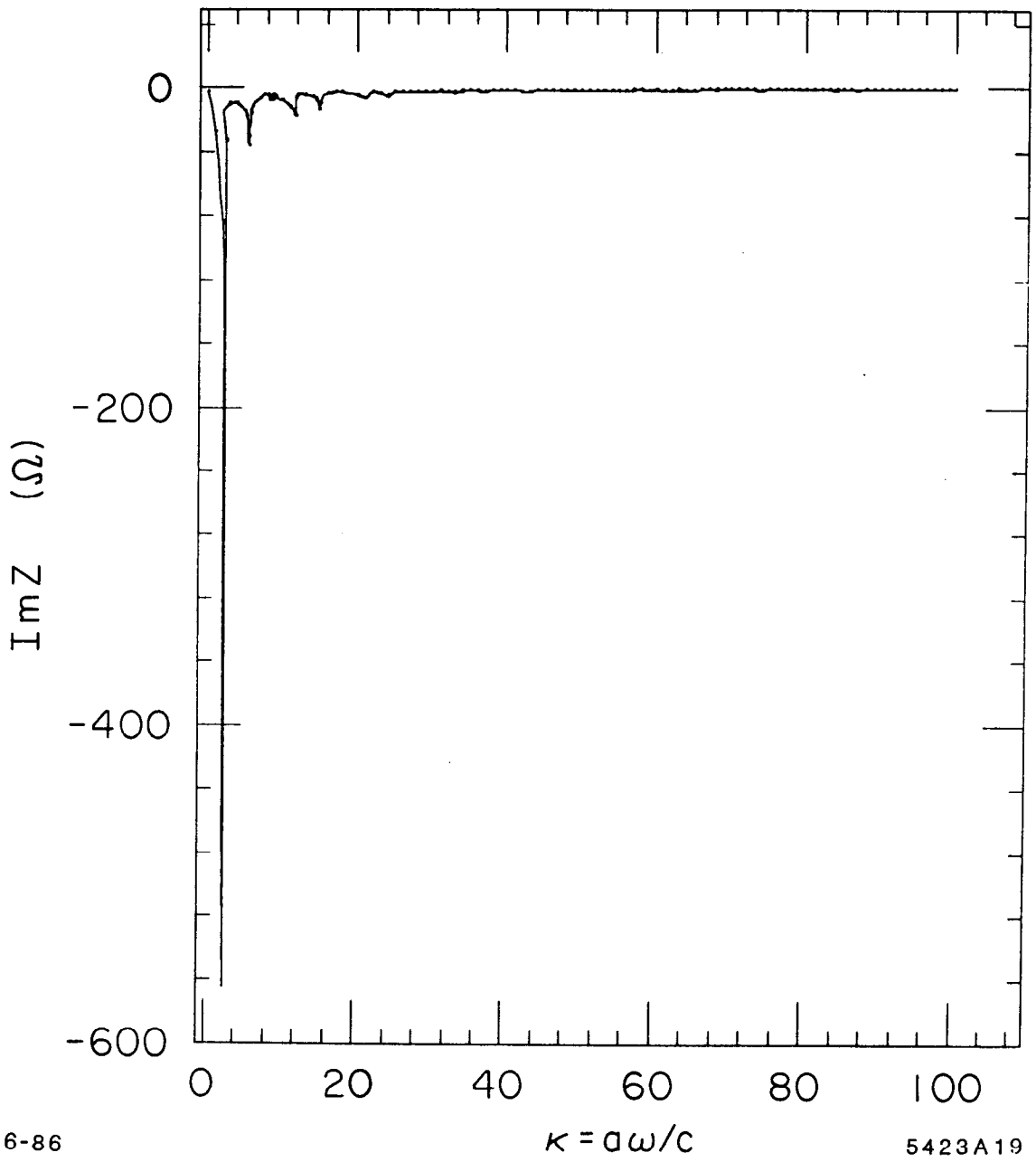

Fig. 16

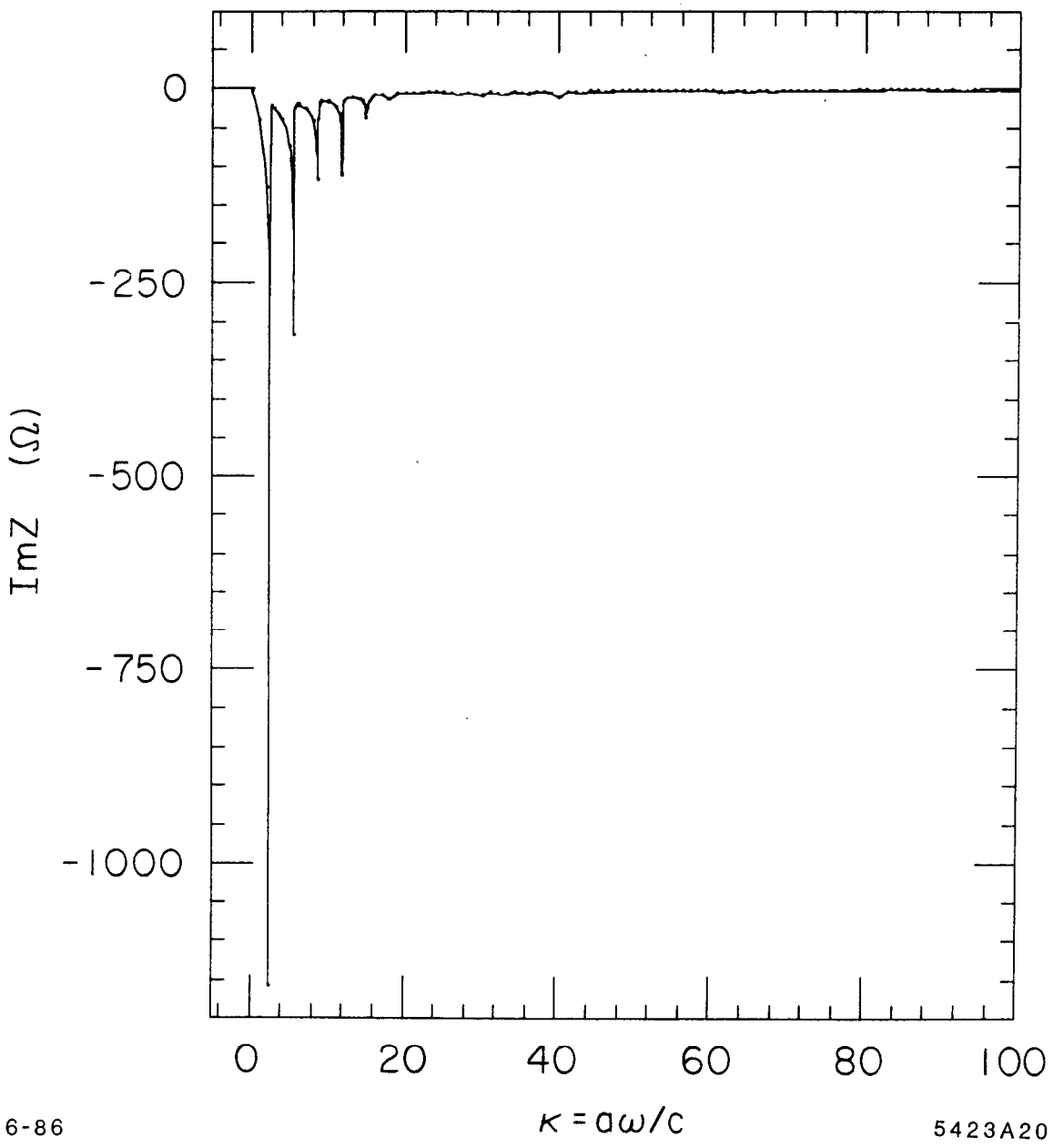

Fig. 17

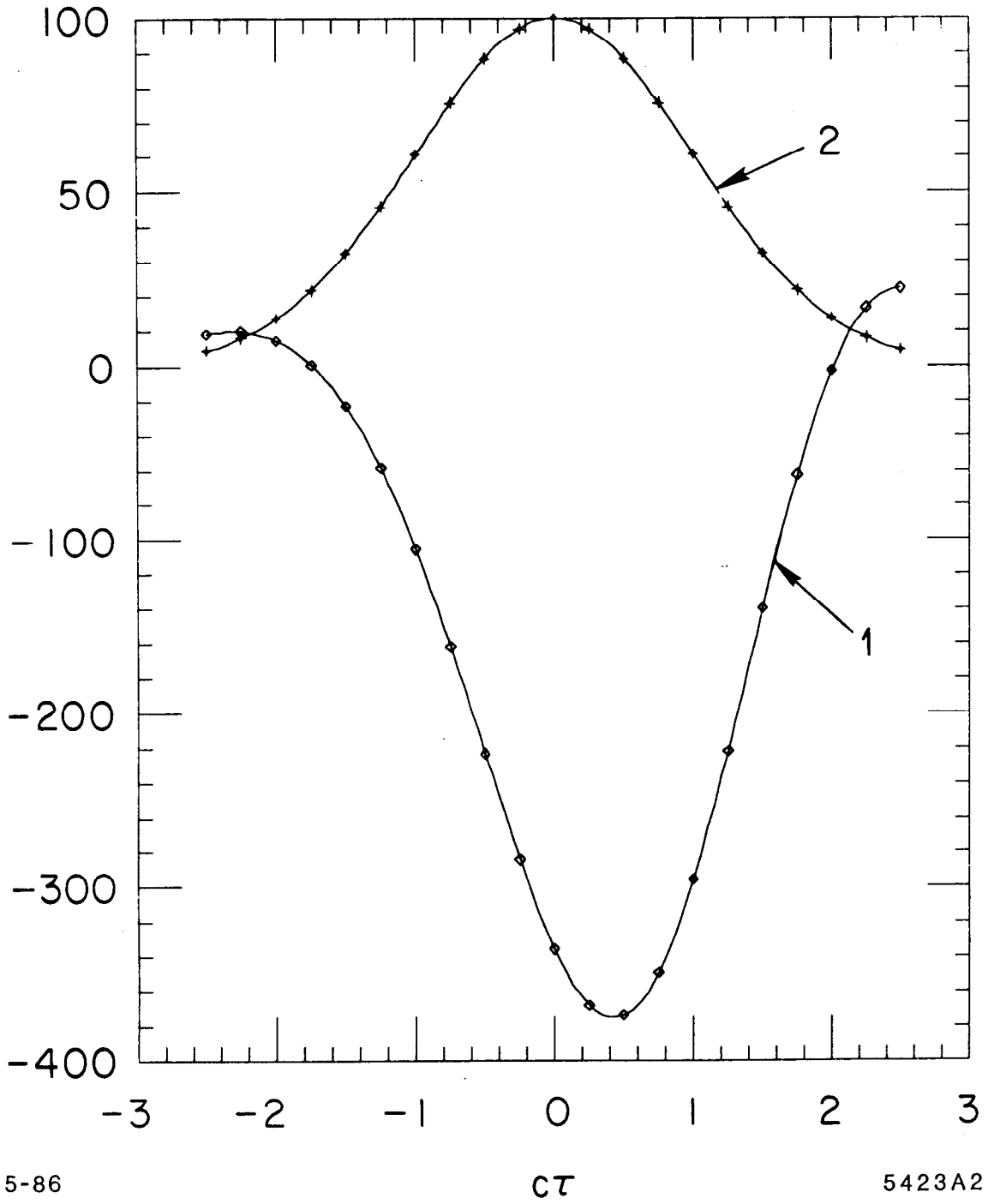

Fig. 18